

De Sitter Special Relativity as a Possible Reason for Conformal Symmetry and Confinement in QCD

Mariana Kirchbach^a and Clifford B. Compean^b

^aInstituto de Física, UASLP, Av. Manuel Nava 6, Zona Universitaria,
San Luis Potosí, S.L.P. 78290, México

^bFacultad de Ciencias, UASLP,
Av. Chapultepec 1570, Privadas del Pedregal,
San Luis Potosí, S.L.P. 78295, México

E-mails: mariana@ifisica.uaslp.mx (*Corresponding author*), cliffor7@gmail.com

Abstract

Conformal symmetry and color confinement in the infrared regime of QCD are interpreted by means of a conjectured deSitter dS_4 geometry of the internal space-time of hadrons, an assumption inspired by the hypothesis on deSitter special relativity. Within such a scenario, the interactions involving the virtual gluon- and constituent quark degrees of freedom of hadrons are deduced from the Green functions of Laplace operators on the dS_4 geodesics. Then the conformal symmetry of QCD emerges as a direct consequence of the conformal symmetry of the dS_4 space-time, while the color confinement, understood as colorlessness of hadrons, appears as a consequence of the inevitable charge neutrality of the unique closed space-like manifold, the three dimensional hyper-sphere S^3 , on whose geodesics the hadron's constituents are conjectured to reside when near rest frame. Mesons are now modelled as quarkish color-anticolor dipoles, whose free quantum motions on the aforementioned S^3 geodesics are perturbed by a potential generated by a gluon-anti-gluon color dipole. The potential predicted presents itself as the color charge analogue to the “curved” Coulomb potential, i.e. to the electric potential that defines a consistent electrostatic theory on a hyper-spherical surface. The advantage of this method is that it allows to establish a direct relationship of the potential parameters to the fundamental constants of QCD. We apply the model to the description of the spectra of the a_1 and f_1 mesons, and the pion electric charge form factor, finding fair agreement with data.

PACS: 03.30.+p (Special relativity), 11.30.-j (Symmetry in theory of fields and particles), 12.38.Aw (Quark confinement)
Key words: deSitter special relativity, conformal symmetry, color confinement, unflavored mesons, strong coupling constant

“Think geometrically, prove algebraically”,
John Torrence Tate Jr.
“...verify experimentally!”
Galileo

Dedicated to the 60th birthday of Prof. Valeri V. Dvoeglazov.
Our wish, an easy going journey through his successful life,
full of valuable goals, achievements, and memories.

1 Introduction

Theoretical models in physics are frequently developed with the aim to explain particular observational data. Such approaches, termed to as “bottom-up”, obviously depend on the data set chosen as the point of departure. It quite might happen that at different energy scales, different models can be adequate. For example, at low-, up to pretty high energies, the electron charge in the Quantum Electrodynamics (QED) can be considered as a constant, but in very strong electromagnetic fields, generated in the interiors of stars, and in collisions, it can become dependent on the transferred momentum. Particles interacting via the so called “strong” interactions, the hadrons, are described in analogy to QED by a properly designed fundamental gauge theory, the Quantum Chromodynamics (QCD), named in this way in reference to the hypothesis that the hadron constituents, the quarks, are endowed with three different degrees of freedom, conditionally termed to as red-, blue-, and green “color charges”. All strong interacting systems observed so far have been found to be color-neutral, a phenomenon known as color-non-observability, or, color confinement. The phenomenon has been built

into the fundamental gauge theory of strong interactions through a special choice of the gauge group, $SU(3)_c$, which first prescribes the number of “colored” gauge fields, the gluons, to be eight, and then “locks” all the color degrees of freedom, through limiting the irreducible representations to those of the factor group with respect to the central charges, $SU(3)_c/Z_3$. The space-time wave equations following from QCD are differential equations of high order and difficult to tackle. For the immediate analyzes of the rapidly accumulating data on hadrons concerning their masses, decay modes, collision probabilities (scattering cross sections), compiled in [1], a model has been developed, the “constituent” quark model which is based on second order differential equations of the Sturm-Liouville type, equivalent to employing potentials in the quantum mechanical wave equations of Schrödinger-, Klein-Gordon-, or Dirac. Historically, as point of departure for the traditional quark model [2] have served the hadrons of the lowest masses, the pseudo-scalar mesons η , π (pion), and K (kaon), on the one side, and the spin-1/2 baryons, the nucleon N , the Σ , and Ξ hyperons, as well as their spin-3/2 excitations Δ , Σ^* , and Ξ^* , supplemented by the Ω -Hyperon, on the other. The potentials of conventional use employed so far within this framework have been predominantly power functions of relative distances. As a rule, the quark models can not be directly linked to the gauge theory of strong interactions, possibly with the exception of the MIT bag model [3], and versions of it [4]. To the best of our knowledge, none of the conventional constituent quark models has provided hints on possible reasons behind the confinement, nor enabled extraction from data on spectra of the value of the fundamental QCD coupling. In a recent work of ours [5], the choice of the data set to be explained by a “bottom-up” quark model has been shifted from the lowest to the highest masses of the unflavored mesons which are of the order of 2300 MeV. The phenomenon to be explained there referred to the observed striking hydrogen-like degeneracies between states distinct through their spins but of same isospin (number of states with different electric charges), and same CP quantum numbers (the product of spatial (P), and charge conjugation (C) parities). The explanation suggested was based on two fundamental principles. We assumed validity of,

- deSitter dS_4 special relativity [6],
- interactions defined by Laplacians on geometric manifolds [7].

According to the first principle,

- the space-time in which the material bodies, in our case the hadrons, are propagating in real time, and that corresponds to the “external space-time”, is described by means of all the events placed in the interiors of all Minkowski’s light cones, constructed for anyone of the local observers on the four-dimensional dS_4 hyperboloid of one shell, \mathbf{H}_1^4 , via its intersections by 4D planes passing parallel to the symmetry axis and containing the observer’s location,
- the space-time in which the virtual bodies, in our case the quark and gluon constituents of the hadrons, can interact instantaneously, and that corresponds to the “internal space-time”, is described by means of all the events placed outside of the aforementioned light cones.

According to the second principle, fundamental interactions are defined by Green functions of Laplace operators on manifolds, the latter being hypothesized by us to be suitably chosen dS_4 geodesics.

The principle advantage of fixing the geometry of the internal space-time of hadrons to the dS_4 hyperboloid is that among its rich geodesic structure there exists in particular one geodesic space that inevitably and necessarily describes a confinement phenomenon akin to the color charge neutrality in QCD. This is the unique closed space-like hyper-spherical manifold, S^3 , located at the “waist” of the hyperboloid.

Indeed, it can be shown that the Gauss theorem and the superposition principle allow only charge neutral configurations to exist on such a surface, the lowest configurations being charge dipoles. Moreover, free quantum motions of quark-anti-quark dipoles on S^3 , when perturbed by the potential generated by a gluon-anti-gluon dipole, give rise to an instantaneous interaction capable of explaining a large amount of data on the reported meson excitations [5], [8]. To be specific, the aforementioned interaction presents itself as the color charge analogue to the “curved” Coulomb potential on S^3 , given by [9]

$$V_C^{S^3} = \frac{\ell(\ell+1)}{\sin^2 \frac{\widehat{r}}{R}} - \alpha Z \cot \frac{\widehat{r}}{R} \xrightarrow{R \rightarrow \infty} V_C^{E_3} = R^2 \frac{\ell(\ell+1)}{r^2} - R \frac{\alpha Z}{r}, \quad (1)$$

where R is the S^3 hyper-radius, \widehat{r} denotes the arc of the geodesic (to be specified below) while $V_C^{E_3}$ is the standard Coulomb potential in flat three dimensional Euclidean space, E_3 , the limiting $V_C^{S^3}$ case for $R \rightarrow \infty$. Then, the strong interaction under discussion is obtained from $V_C^{S^3}$ by replacing the product, αZ , of the fundamental constant α in QED,

and the charge number, Z , by $\alpha_s N_c$, the product of the strong coupling α_s in QCD and the number of color charges, N_c . The strong interaction potential derived in this way allows one to put the description of mesons, the simplest (two-body) composite system in QCD, at comparable footing with that of the H Atom, the simplest (two-body) system in QED. In fitting by the above potential data on the observed degeneracy patterns of the unflavored meson spectra, predictions for α_s at different meson masses could be obtained in [8] that matched values reported by other sources. In [10] the method under discussion has been further successfully tested in the evaluation of the nucleon electromagnetic form-factors.

In the present study we first briefly review the proposal of [5], [8] and then put it at work in the description of the previously not considered a_1 and f_1 meson spectra, and also in the explanation of the pion electric charge form factor, finding very satisfactory agreement with data.

The article is structured as follows. In the next section we highlight the idea of [6] on the extension of Einstein's special relativity to deSitter relativity. In section 3 we recall the elements of the algebraic description of the deSitter geometry, which allows us to consider there free quantum motions on the unique closed hyper-spherical space-like manifold, as well as on open hyperbolic time-like geodesics. In section 4 we transform the aforementioned free motions into one-dimensional quantum mechanical wave equations with the respective trigonometric Scarf well-, and the hyperbolic Pöschl-Teller barrier potentials. There, we present a scenario for a duality between the descriptions of hadrons as states bound within the Scarf potential, on the one side, and as resonances transmitted through the Pöschl-Teller barrier, on the other, two methods suited for handling particle physics phenomena in low- and high-energy regimes. In section 5 we explore consequences of the innate charge neutrality of the hyper-sphere on the internal structure of systems on this space and review the prediction of [5] on a confinement phenomenon. In section 6 we associate the predicted confinement phenomenon with the experimentally detected color confinement in QCD and analyze data on the f_1 and a_1 mesons, together with the pion electric charge form factor, before closing by a short Conclusion section.

2 The Geometric Ansatz. Immersing Minkowski- into deSitter space-time

All theoretical descriptions of processes in the micro-world have to obey the theory of Special Relativity which requires the values of the physical observables to be same in all reference frames related to each other by Lorentz transformations, known to conserve the “intervals”, s^2 , in a Minkowskian space-time, \mathcal{M}_{1+3} , of one time-like (ct) and three space-like (\mathbf{r}) dimensions according to,

$$\mathcal{M}_{1+3} : \quad c^2(t_1 - t_2)^2 - (x_1 - x_2)^2 + (y_1 - y_2)^2 + (z_1 - z_2)^2 = s^2, \quad s^2 \gtrless 0. \quad (2)$$

Here, x_i, y_i , and z_i (with $i = 1, 2$) are the Cartesian position coordinates of two bodies in the ordinary three-dimensional Euclidean space, E_3 , while t_1 and t_2 are in turn their time coordinates, and c is the speed of light.

The intervals in (2) for $s^2 > 0$ can be viewed as locuses of points lying on three dimensional hyperboloids of two sheets, denoted by \mathbf{H}_{\pm}^3 , encapsulated inside the “null hyperboloid”, $c^2 t^2 - \mathbf{r}^2 = 0$, a cone also termed to as the “Light Cone”, as schematically illustrated in Fig. 1. The null-intervals remain invariant under five more transformations termed to as “conformal”, the resulting symmetry being the “kinematic conformal symmetry” [11]. The conformal symmetry is associated with all the transformations which leave the interval, $ds^2 = g_{\mu\nu}(x)dx^\mu dx^\nu$, invariant, modulo a multiplicative “conformal factor” of $e^{\omega(x)}$.

In Special Relativity it is argued that the hyperboloids inside the upper part of the cone describe the causal “Future” while those of the bottom part describe the causal “Past”. The meaning of “causal” is that events in these regions describe material bodies moving with subluminal velocities, because their time-orderings are preserved by all Lorentz transformations and thus allow one to define the arrow of time in this domain. In contrast, the surrounding hyperboloids of one sheet represent the acausal region, where no arrow of time can be defined because here Lorentz transformations can change the time-orderings of the events. Such events can be used only in the description of virtual degrees of freedom of the material bodies, such as their constituents, among them the nucleons in a nucleus, the quarks and gluons in hadrons etc.

Measurements in physics can be carried out only on material bodies, as described by means of events located in the causal region, the processes being termed to as “real”, or “on mass-shell”, in reference to the definition of the invariant mass, M , by means of the so called “on-mass shell” relation, $E^2 - \mathbf{p}^2 c^2 = M^2 c^4$, between the energy, E , and linear

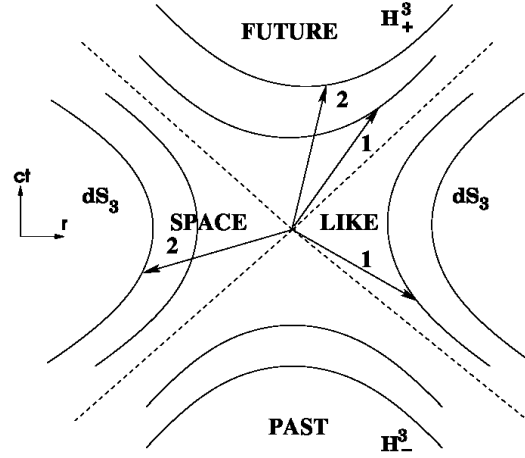


Figure 1: Schematic presentation of Minkowski's space time, reduced to a plane. Two examples of moved reference frames are given and their axes labeled by "1", and "2". The axes of a frame in motion do not remain mutually orthogonal, the angles between them being dependent on the velocity. A fixed interval, $s^2 > 0$, defines a three-dimensional hyperboloid of a vertical time-like symmetry axis and of two-sheets represented by the hyperbola of two branches on the figure, marked by \mathbf{H}_+^3 and \mathbf{H}_-^3 , respectively, or, of one sheet, a so called deSitter dS_3 space-time, for $s^2 < 0$. The dashed lines mark the null-hyperboloid (light cone) corresponding to $s^2 = 0$.

momentum, \mathbf{p} . Instead, the constituents of the material bodies and their instantaneous interactions are exclusively described by means of events located in the domain outside the light cone. Notice that the causal and acausal regions are disconnected and described by means of independent coordinates, a reason for which transformations and operators from the two regions are commuting with each other.

Thinking now geometrically, one can ask the question, posed in [6], on the type of physics one could encounter by imagining the light cone and the enclosed \mathbf{H}_\pm^3 hyperboloids immersed locally into a four-dimensional hyperboloid of one sheet as schematically represented in Fig. 2. Stated differently, one could entertain the idea of extending the inaccessible to direct measurements space-like region of the Minkowski space-time by one extra space-like (infinite) dimension, x_4 , and requiring outside the causal region invariance of the larger intervals,

$$dS_4 : \quad c^2 t^2 - \mathbf{r}^2 - x_4^2 = S^2, \quad S^2 = -R^2 < 0. \quad (3)$$

Here, R is a new real length parameter. A space-time defined in this way is known under the name of "four-dimensional deSitter space-time", abbreviated, dS_4 . It represents a four dimensional hyperboloid of one sheet, denoted by \mathbf{H}_1^4 , with the time line as a symmetry axis. Within this set up, causal hyperboloids in Einstein's special relativity correspond to so called causal patches on dS_4 obtained through intersections (slicings) of \mathbf{H}_1^4 by four-dimensional planes parallel to the time axis as depicted in Figure 2. The interval in (3) is conserved besides under Lorentz transformations also under transformations which ensure the transitivity of the dS_4 space-time and combine in a particular way translations with four of the five conformal transformations, the so called special conformal transformations, a reason for which dS_4 features conformal symmetry [6]. In the following we will explore consequences of this idea.

3 Building up the algebraic description of the dS_4 geometry

In this section, which partially follows our previous work [5], we recall once again the usefulness of the dS_4 geometry for quantum physics. For this purpose we start building up the algebraic description of quantum motions there, beginning with free motions. Free quantum motions on any space-time are described by the eigenmodes of the kinetic energy

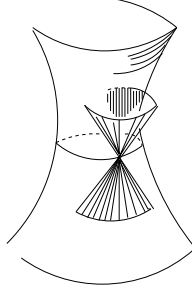


Figure 2: Schematic illustrative presentation of a causal Minkowski light cone relevant to a local observer placed at the “waist” of the dS_4 hyperboloid, for concreteness.

operator there, given by the respective Laplacian. On dS_4 , parameterized in global coordinates as [12],

$$\begin{aligned}
 x^0 &= R \sinh \rho, \quad \rho \in (-\infty, +\infty), \\
 x^4 &= R \cosh \rho \sin \chi, \quad \chi \in \left[-\frac{\pi}{2}, +\frac{\pi}{2}\right], \\
 x^1 &= R \cosh \rho \cos \chi \sin \theta, \quad \theta \in \left[-\frac{\pi}{2}, +\frac{\pi}{2}\right], \\
 x^2 &= R \cosh \rho \cos \chi \cos \theta \sin \varphi, \quad \varphi \in [0, 2\pi], \\
 x^3 &= R \cosh \rho \cos \chi \cos \theta \cos \varphi,
 \end{aligned} \tag{4}$$

one encounters the Laplacian, denoted by $\Delta_{dS_4}(\rho, \chi, \theta, \varphi)$ as,

$$\Delta_{dS_4}(\rho, \chi, \theta, \varphi) = \frac{1}{R^2 \cosh^3 \rho} \frac{\partial}{\partial \rho} \cosh^3 \rho \frac{\partial}{\partial \rho} + \frac{\mathcal{K}^2(\chi, \theta, \varphi)}{R^2 \cosh^2 \rho}. \tag{5}$$

The $\mathcal{K}^2(\chi, \theta, \varphi)$ part of $\Delta_{dS_4}(\rho, \chi, \theta, \varphi)$ in (5) stands for the squared four dimensional (4D) angular momentum operator,

$$\mathcal{K}^2(\chi, \theta, \varphi) = -R^2 \Delta_{S^3}(\chi, \theta, \varphi) = -\frac{1}{\cos^2 \chi} \frac{\partial}{\partial \chi} \cos^2 \chi \frac{\partial}{\partial \chi} + \frac{\mathbf{L}^2(\theta, \varphi)}{\cos^2 \chi}, \tag{6}$$

where $\Delta_{S^3}(\chi, \theta, \varphi)$ is the Laplace operator on the unique closed space-like manifold [14] on dS_4 which is a three dimensional hyper-sphere, S^3 , of (hyper)radius R . The $\Delta_{S^3}(\chi, \theta, \varphi)$ eigenmodes are determined by the hyper-spherical harmonics, $Y_{K\ell m}(\chi, \theta, \varphi)$, as

$$-\hbar^2 c^2 \Delta_{S^3}(\chi, \theta, \varphi) Y_{K\ell m}(\chi, \theta, \varphi) = \frac{\hbar^2 c^2}{R^2} K(K+2) Y_{K\ell m}(\chi, \theta, \varphi), \quad |m| \in [0, \ell], \tag{7}$$

explicitly given by,

$$Y_{K\ell m}(\chi, \theta, \varphi) = \mathcal{S}_{n\ell}(\chi) Y_\ell^m(\theta, \varphi), \tag{8}$$

$$\mathcal{S}_{n\ell}(\chi) = \cos^\ell \chi \mathcal{G}_n^{\ell+1}(\sin \chi), \quad n = K - \ell. \tag{9}$$

Here, $\mathcal{G}_n^{\ell+1}(\sin \chi)$, and $Y_\ell^m(\theta, \varphi)$ in turn denote the Gegenbauer polynomials, and the ordinary spherical harmonics. They describe rigid “dumbbells” (“rotators”) in four Euclidean dimensions, freely hovering around their mass centers, with the ends tracing S^3 great circles.

The free waves of the dS_4 Laplacian in (5) are then described in terms of 5D pseudo-spherical harmonics, denoted by $Y_{\bar{K}K\ell m}(\rho, \chi, \theta, \varphi)$, the solutions to,

$$-\hbar^2 c^2 \Delta_{dS_4}(\rho, \chi, \theta, \varphi) Y_{\bar{K}K\ell m}(\rho, \chi, \theta, \varphi) = -\frac{\hbar^2 c^2}{R^2} \bar{K}(\bar{K}+3) Y_{\bar{K}K\ell m}(\rho, \chi, \theta, \varphi), \tag{10}$$

and are defined as,

$$Y_{\bar{K}K\ell m}(\rho, \chi, \theta, \varphi) = \phi_{\bar{K}}(\rho) Y_{K\ell m}(\chi, \theta, \varphi), \quad \bar{K}, K = 0, 1, 2, \dots, \quad \ell = 0, 1, 2, \dots, K, \quad (11)$$

where \bar{K} and K can take all non-negative integer values.

Here, the $\phi_{\bar{K}}(\rho)$ functions express in terms of Jacobi's polynomials, $P_{n_r}^{ab}(x)$, of equal real parameters, and a pure imaginary argument according to,

$$\phi_{\bar{K}}(\rho) = \cosh^{-\frac{a}{2}-\frac{3}{2}} \rho P_{n_r}^{-a-\frac{1}{2}, -a-\frac{1}{2}}(i \sinh \rho), \quad (12)$$

$$a = \frac{1}{2} + (K + 1), \quad (13)$$

$$P_{n_r}^{-a-\frac{1}{2}, -a-\frac{1}{2}}(i \sinh \rho) = \frac{(-a + \frac{1}{2})_n}{n_r!} {}_2F_1 \left(-n_r, n_r - 2a; -a + \frac{1}{2}; \frac{1 - i \sinh \rho}{2} \right). \quad (14)$$

Furthermore, ${}_2F_1$ is the hyper-geometric function, $(\dots)_t$ is the Pochhammer symbol, ρ is the arc of an open time like hyperbolic geodesic on dS_4 , and n_r denotes the polynomial degree.

In summary, the equations (10) and (7) describe free quantum motions along the respective open time-like and closed space-like geodesics on dS_4 in the sense that the arguments of the wave functions $\phi_{\bar{K}}(\rho)$, and $\mathcal{S}_{\ell n}(\chi)$ in the respective equations (12) and (9), change along the arcs, $R\rho$, and $R\chi$, of great circles on such geodesics. The open time-like geodesics considered here are hyperbolic deSitter space-times of one less dimension, i.e. dS_3 space-times, while the unique closed space-like geodesic is a three dimensional (hyper)spherical surface S^3 located at the “waist” of the dS_4 hyperboloid.

4 From free quantum motions on dS_4 to one-dimensional stationary wave equations with centrifugal potentials

The free quantum motions on the open time-like-, and the closed space-like dS_4 geodesics can be transformed in their turn into stationary quantum mechanical wave equations with the one-dimensional hyperbolic Pöschl-Teller potential, $V_{\text{PT}}(\rho)$, and the trigonometric Scarf potential, $V_{\text{Sc}}(\chi)$.

4.1 Quantum motions on open time-like geodesics and the hyperbolic Pöschl-Teller barrier

To prove the aforementioned statement, the following variable change in (12) has to be performed,

$$F_{\bar{K}n_r}(\rho) = \cosh^{\frac{3}{2}} \rho \phi_{\bar{K}}(\rho), \quad \bar{K} = K - n_r, \quad (15)$$

in which case the equation (10) is similarity transformed toward,

$$\begin{aligned} -\hbar^2 c^2 \left[\cosh^{\frac{3}{2}} \rho \Delta_{dS_4}(\rho, \chi, \theta, \varphi) \cosh^{-\frac{3}{2}} \rho \right] &= \left[\cosh^{\frac{3}{2}} \rho Y_{\bar{K}K\ell m}(\rho, \chi, \theta, \varphi) \right] \\ &= -\frac{\hbar^2 c^2}{R^2} \bar{K}(\bar{K} + 3) \left[\cosh^{\frac{3}{2}} \rho Y_{\bar{K}K\ell m}(\rho, \chi, \theta, \varphi) \right]. \end{aligned} \quad (16)$$

Introducing now the notation, $\mathcal{H}_{\text{PT}}(\rho, \chi, \theta, \varphi)$, for the Laplacian, $[-\hbar^2 c^2 \Delta_{dS_4}(\rho, \chi, \theta, \varphi)]$, upon its similarity transformation by the $\cosh^{\frac{3}{2}} \chi$ function,

$$\mathcal{H}_{\text{PT}}(\rho, \chi, \theta, \varphi) = \cosh^{\frac{3}{2}} \rho \left[-\hbar^2 c^2 \Delta_{dS_4}(\rho, \chi, \theta, \varphi) \right] \cosh^{-\frac{3}{2}} \rho, \quad (17)$$

and making use of (5) and (11), the equation (16) equivalently rewrites as,

$$\begin{aligned} \mathcal{H}_{\text{PT}}(\rho, \chi, \theta, \varphi) F_{\bar{K}n_r}(\rho) Y_{K\ell m}(\chi, \theta, \varphi) &= \frac{\hbar^2 c^2}{R^2} \left[-\frac{d^2}{d\rho^2} + V_{\text{PT}}(\rho) + \frac{3^2}{2^2} \right] \mathbf{I}(\chi, \theta, \varphi) \\ &\times F_{\bar{K}n_r}(\rho) Y_{K\ell m}(\chi, \theta, \varphi) \\ &= -\frac{\hbar^2 c^2}{R^2} \bar{K}(\bar{K} + 3) F_{\bar{K}n_r}(\rho) Y_{K\ell m}(\chi, \theta, \varphi). \end{aligned} \quad (18)$$

Here, $\mathbf{I}(\chi, \theta, \varphi)$ is the identity operator in the $S^3(\chi, \theta, \varphi)$ subspace, $V_{\text{PT}}(\rho)$ stands for the Pöschl-Teller (PT) potential given by,

$$\mathcal{V}_{\text{PT}}(\rho) = \left[(K+1)^2 - \frac{1}{4} \right] \text{sech}^2 \rho, \quad \rho \in (-\infty, +\infty). \quad (19)$$

Notice that the similarity transformation conserves the $[-\hbar^2 c^2 \Delta_{dS_4}(\rho, \chi, \theta, \varphi)]$ eigenvalues in (10). A way of rephrasing the similarity transformation is to cast it in the form of an intertwining by the $\cosh^{\frac{3}{2}} \rho$ function of $\mathcal{H}_{\text{PT}}(\rho, \chi, \theta, \varphi)$ with the $[-\hbar^2 c^2 \Delta_{dS_4}(\rho, \chi, \theta, \varphi)]$ Laplacian according to,

$$-\hbar^2 c^2 \cosh^{\frac{3}{2}} \rho \Delta_{dS_4}(\rho, \chi, \theta, \varphi) = \mathcal{H}_{\text{PT}}(\rho, \chi, \theta, \varphi) \cosh^{\frac{3}{2}} \rho, \quad (20)$$

and to recall that intertwined Hamiltonians are isospectral [13]. Also notice that the PT potential can be equivalently rewritten to,

$$\mathcal{V}_{\text{PT}}(\rho) = \left[(K+1)^2 - \frac{1}{4} \right] \frac{1}{\cosh^2 \rho} = - \left[(K+1)^2 - \frac{1}{4} \right] \tanh^2 \rho + \frac{\hbar^2 c^2}{R^2}, \quad (21)$$

where the potential on the r.h.s. is known under the name of the “Higgs oscillator” on dS_4 in reference to the fact that the leading term in the series expansion of $\tanh^2 \rho$ goes as the square, ρ^2 , of the argument meaning that to leading order the hyperbolic Pöschl-Teller potential behaves as an oscillator. In this sense, free motions on the open hyperbolic time-like geodesics on dS_4 can be viewed as “Higgs” oscillations. An interesting phenomenon that can be related to free quantum motion on the dS_4 space is predicted upon the complexification, $(K+1) \rightarrow i(K+1)$, of the parameter defining the potential strength in (19), equivalently, upon the analytical continuation of the four-dimensional angular momentum to complex values. In this case $\mathcal{V}_{\text{PT}}(\rho)$ is transformed into a barrier and one can consider the complex energies of the resonances transmitted through it. To do so, one has to calculate the transmission scattering matrix, $T(k)$. A scheme for such a calculation has been presented in detail in [15]. The expression obtained along the lines of [15] for the case of our interest reads,

$$T(k) = \frac{\sinh^2 \pi k}{\cosh^2 \pi k + \sinh^2 \pi (K+1)}. \quad (22)$$

Then the poles, which appear at $k = [(K+1) + i(n_r - \frac{1}{2})]$, define the squared complex energies, $(\mathcal{E}^{(res)})^2$, of the resonances transmitted through the barrier as [5],

$$(\mathcal{E}^{(res)})^2 = \frac{\hbar^2 c^2}{R^2} k^2, \quad \text{Im} \left(\mathcal{E}^{(res)} \right)^2 = 2 \frac{\hbar^2 c^2}{R^2} (K+1) \left(n_r - \frac{1}{2} \right). \quad (23)$$

$$\begin{aligned} \text{Re} \left(\mathcal{E}^{(res)} \right)^2 - c_0 &= \frac{\hbar^2 c^2}{R^2} (K+1)^2, \\ c_0 &= -\frac{\hbar^2 c^2}{R^2} \left(n_r - \frac{1}{2} \right)^2 + A^2, \end{aligned} \quad (24)$$

where A^2 is some additive ad hoc constant which on long term could be helpful in adjustments of the potential parameters to data. Let us interpret the real parts of the squared complex energies, $\left[\text{Re} \left(\mathcal{E}^{(res)} \right)^2 - c_0 \right]$, at the poles of $T(k)$, as a squared invariant mass M^2 , i.e. let us set,

$$M^2 \equiv \text{Re} \left(\mathcal{E}^{(res)} \right)^2 - c_0 = \frac{\hbar^2 c^2}{R^2} (K+1)^2 = \frac{\hbar^2 c^2}{R^2} (n + \ell + 1)^2, \quad K = n + \ell. \quad (25)$$

The expression gives rise to linear “trajectories” (linear dependencies of the angular momentum on the mass) of the art,

$$\ell = \alpha(R)M - n - 1, \quad \ell = 0, 1, 2, \dots, \quad \ell + n = K, \quad K = 0, 1, 2, \dots \quad (26)$$

with n being the number of nodes in the Gegenbauer polynomials in (9).

4.2 Quantum motion on the closed space-like hyper-spherical geodesics and the trigonometric Scarf potential

In a similar way, through the variable change,

$$\begin{aligned}\cos \chi Y_{K\ell m}(\chi, \theta, \varphi) &= \cos \chi \mathcal{S}_{n\ell}(\chi) Y_{\ell m}(\theta, \varphi) \\ &= U_{n\ell}(\chi) Y_{\ell}^m(\theta, \varphi), \quad U_{n\ell}(\chi) = \cos \chi \mathcal{S}_{n\ell}(\chi),\end{aligned}\tag{27}$$

with $\mathcal{S}_{n\ell}(\chi)$ from (9), the equation (7) is similarity transformed toward,

$$\begin{aligned}-\hbar^2 c^2 [\cos \chi \Delta_{S^3}(\chi, \theta, \varphi) \cos^{-1} \chi] &[\cos \chi Y_{K\ell m}(\chi, \theta, \varphi)] \\ &= \frac{\hbar^2 c^2}{R^2} K(K+2) [\cos \chi Y_{K\ell m}(\chi, \theta, \varphi)].\end{aligned}\tag{28}$$

In now introducing the notation, $\mathcal{H}_{\text{Sc}}(\chi, \theta, \varphi)$, for the Laplacian, $[-\hbar^2 c^2 \Delta_{S^3}(\chi, \theta, \varphi)]$, upon its similarity transformation by the $\cos \chi$ function,

$$\mathcal{H}_{\text{Sc}}(\chi, \theta, \varphi) = -\hbar^2 c^2 [\cos \chi \Delta_{S^3}(\chi, \theta, \varphi) \cos^{-1} \chi],\tag{29}$$

making use of (8), (9), and (6), and upon some algebraic manipulations, the equation (29) equivalently rewrites as,

$$\begin{aligned}H_{\text{Sc}}(\chi, \theta, \varphi) U_{\ell n}(\chi) Y_{\ell m}(\theta, \varphi) &= \frac{\hbar^2 c^2}{R^2} \left(-\frac{d^2}{d\chi^2} + V_{\text{Sc}}(\chi) - 1 \right) \otimes \mathbf{I}(\theta, \varphi) U_{\ell n}(\chi) Y_{\ell m}(\theta, \varphi) \\ &= \frac{\hbar^2 c^2}{R^2} K(K+2) U_{\ell n}(\chi) Y_{\ell m}(\theta, \varphi),\end{aligned}\tag{30}$$

where $\mathbf{I}(\theta, \varphi)$ is the identity operator on the $S^2(\theta, \varphi)$ subspace of $S^3(\chi, \theta, \varphi)$, and $V_{\text{Sc}}(\chi)$ is the trigonometric Scarf potential

$$V_{\text{Sc}}(\chi) = \ell(\ell+1) \sec^2 \chi, \quad \chi \in \left[-\frac{\pi}{2}, +\frac{\pi}{2} \right].\tag{31}$$

Notice that the barrier potential in (19) can be obtained from the well potential in (31) through complexification of the argument, modulo multiplicative constant.

Same as in the case of the dS_4 Laplacian, also the similarity transformation of the S^3 Laplacian conserves its eigenvalues in (7) and because these eigenvalues are bound from below, they are referred to as the Laplacian's "spectrum".

A way of rephrasing the similarity transformation in (29) is to cast it in the form of an intertwining by the $\cos \chi$ function of $\mathcal{H}_{\text{Sc}}(\chi, \theta, \varphi)$ and the $[-\hbar^2 c^2 \Delta_{S^3}(\chi, \theta, \varphi)]$ Laplacian according to

$$-\hbar^2 c^2 \cos \chi \Delta_{S^3}(\chi, \theta, \varphi) = \mathcal{H}_{\text{Sc}}(\chi, \theta, \varphi) \cos \chi,\tag{32}$$

and recall isospectrality of intertwined operators known from the super-symmetric quantum mechanics [13]. The considerations from above show that in terms of one-dimensional wave equations, the free quantum motions along the open time-like, and the closed space-like dS_4 geodesics give in turn rise to the hyperbolic Pöschl-Teller, $V_{\text{PT}}(\rho)$, equivalently, the Higgs oscillator on dS_4 , and the trigonometric Scarf, $V_{\text{Sc}}(\chi)$ potential, which are well known from the super-symmetric quantum mechanics [13] to be exactly solvable. More important, the Hamiltonians $\mathcal{H}_{\text{PT}}(\rho, \chi, \theta, \varphi)$ and $\mathcal{H}_{\text{Sc}}(\chi, \theta, \varphi)$, in being intertwined with the respective dS_4 and S^3 Laplacians, conserve the symmetry of the free geodesic motions which is the conformal symmetry, a reason for which the one dimensional potentials in (19)-(21), and (31) are said to be conformal. Such occurred because the latter potentials correspond to "centrifugal" terms on the respective hyperbolic and hyper-spherical manifolds. We now rename by $\left(\mathcal{E}^{(\text{bound})} \right)^2$ the $H_{\text{Sc}}(\chi, \theta, \varphi)$ eigenvalues in (30), i.e. we introduce the notation,

$$\left(\mathcal{E}^{(\text{bound})} \right)^2 = \frac{\hbar^2 c^2}{R^2} (K+1)^2, \quad K = n + \ell.\tag{33}$$

Because the energy depends on the K quantum number alone, and due to the branching rules,

$$\ell \in [0, K], \quad |m| \in [0, \ell], \quad (34)$$

as explained in the equation (11), one immediately notices that the levels of the trigonometric Scarf potential are $\sum_{\ell=0}^K (2\ell + 1) = (K + 1)^2$ -fold degenerate. This type of degeneracy is known from the Hydrogen Atom, where it is attributed to the conformal symmetry of the Maxwell equations, or, more general, to the conformal symmetry of the Relativistic Electrodynamics [16]. Therefore, the eigenmodes of the free quantum motion along the closed S^3 hyper-spherical geodesics on dS_4 fall into a conformal spectrum.

4.3 Equality between the masses of the resonances transmitted through the hyperbolic Pöschl-Teller barrier and the excitation energies of the states bound within the trigonometric Scarf potential

Comparison of the real parts of the complex masses of the resonances transmitted through the Pöschl-Teller barrier in (25) with the real excitation energies of the states bound within the trigonometric Scarf potential in (33) reveals their equality as,

$$M^2 = \mathcal{R}e \left(\mathcal{E}^{(res)} \right)^2 = \frac{\hbar^2 c^2}{R^2} (K + 1)^2. \quad (35)$$

Within the geometric context pursued through the text, the duality between the mass-formulas in (26) and (33), translates into duality between quantum motions on open hyperbolic time-like, and the closed hyper spherical space-like geodesics on dS_4 .

In conclusion, with the aid of the dS_4 structure of the domain located outside the causal Minkowski light cones, hypothesized by us to provide the relevant geometry of internal space-time, and employed in the definition of interactions, a pair of potentials could be encountered with the remarkable properties that the real energies of the states bound within the Scarf well potential equal the real parts of the complex energies of the resonances transmitted to the Pöschl-Teller barrier. Moreover, these energies carry same hydrogen-like degeneracies.

In this manner, by virtue of the hypothesis on validity of dS_4 special relativity [6], we were able to establish in [5] a duality between the free quantum motions on open hyperbolic time-like, and closed hyper-spherical space-like geodesics of the dS_4 space-time. To the end of the article, the physical significance of such a duality will be revealed. Before, in the next section, a deeper insight into the physics on the closed hyper-spherical surface S^3 will be gained.

5 Behind the curtains of confinement. Charge neutrality on the hyper-spherical dS_4 geodesics and a conformal color-dipole confining potential

The main point of the present section is to explore consequences of the fact that no single charge can be consistently defined on spheres [17]. Indeed, the lines pouring out of a charge located at a particular point on this space intersect at the antipodal point, creating there a fictitious opposite charge (see Fig. 3). In order to satisfy the Gauss theorem and the principle of superposition on S^3 , fictitious charges have to be avoided and replaced by real charges, thus creating necessarily and inevitably the charge neutrality of the sphere. In order to see this, we recall that the Gauss theorem predicts a $\sec^2 \chi$ functional form [18] for the electric field for $\chi \in [-\pi/2, +\pi/2]$. On the other side, the superposition principle on S^3 predicts same field to be the gradient of the sum of the pod- and anti-pod single charge potentials. In the following we shall show that the E field of a “charge-dipole” (for the time being without specification of the nature of the charge) predicted by the superposition principle on S^3 coincides with the corresponding predictions of the Gauss theorem. In this way we shall prove that a consistent “charge-static” on the hyper-sphere is guaranteed by its charge neutrality.

For this purpose, one needs to know the Laplacian on the complete space-time $R^1 \otimes S^3$, with R^1 standing for the time line, and then to consider it at constant times. This can be done within the framework of the so called Radial Quantization

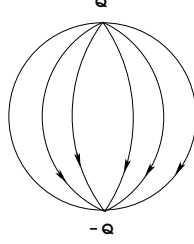


Figure 3: The inevitable charge neutrality of the sphere.

Technique which prescribes to first Wick-rotate via the complexification, $ct \rightarrow ict$, the Minkowski space time of $(1 + 3)$ dimensions to four Euclidean dimensions, switch to global hyper-spherical coordinates, and introduce “time” via the logarithm of the S^3 radius [19]. In so doing one finds the following Laplacian,

$$-\left[\frac{\partial^2}{\partial x_4^2} + \frac{\partial^2}{\partial x_1^2} + \frac{\partial^2}{\partial x_2^2} + \frac{\partial^2}{\partial x_3^2}\right] \longrightarrow -\left[\frac{1}{R^3} \frac{\partial}{\partial R} R^3 \frac{\partial}{\partial R} - \frac{1}{R^2} \mathcal{K}^2(\chi, \theta, \varphi)\right] \quad (36)$$

$$\xrightarrow{R=e^\tau} e^{2\tau} \left[-\frac{\partial^2}{\partial \tau^2} + (\mathcal{K}^2(\chi, \theta, \varphi) + 1)\right]. \quad (37)$$

The τ parameter is known as “conformal time”. To build up charge-statics, one has to set $\tau=\text{const}$ and to calculate the Green function to the remaining piece, the so called conformal Laplacian, $\Delta_{S^3}^1(\chi, \theta, \varphi)$, on S^3 , read off from (37) as

$$\Delta_{S^3}^1(\chi, \theta, \varphi) = \mathcal{K}^2(\chi, \theta, \varphi) + 1, \quad (38)$$

where we have chosen $\tau = 0$, equivalent to $R = 1$. In order to construct the potentials of a charge Q placed at, say, the West “pole”, and of an anti-charge, $(-Q)$, at the East “pole”, one needs to know the respective Green functions, in turn denoted by $\mathcal{G}_{-\frac{\pi}{2}}(\chi)$, and $\mathcal{G}_{+\frac{\pi}{2}}(\chi)$, which have been calculated, among others, in [20], however for $\chi \in [0, \pi]$, and need to be shifted to $\chi \in [-\frac{\pi}{2}, +\frac{\pi}{2}]$. After this small algebraic manipulation, the potentials, constructed from the Green’s function in the standard way known from potential theory [7], emerge as,

$$V_{-\frac{\pi}{2}}(\chi) = Q\mathcal{G}_{-\frac{\pi}{2}}(\chi) = -\frac{Q}{4\pi^2} \left(\chi - \frac{3\pi}{2}\right) \tan \chi, \quad (39)$$

$$V_{+\frac{\pi}{2}}(\chi) = -Q\mathcal{G}_{+\frac{\pi}{2}}(\chi) = -\frac{(-Q)}{4\pi^2} \left(\chi - \frac{\pi}{2}\right) \tan \chi, \quad \chi \in \left[-\frac{\pi}{2}, +\frac{\pi}{2}\right]. \quad (40)$$

In now assuming validity of the superposition principle, one encounters a Charge Dipole (CD) potential to emerge at a point χ on S^3 according to,

$$V_{CD}(\chi) = Q\mathcal{G}_{-\frac{\pi}{2}}(\chi) - Q\mathcal{G}_{+\frac{\pi}{2}}(\chi) = \frac{Q}{4\pi} \tan \chi. \quad (41)$$

The electric field to this dipole is obtained in the standard way through differentiation as,

$$E(\chi) = -\frac{\partial}{\partial \chi} V_{CD}(\chi) = -\frac{Q}{4\pi} \frac{1}{\cos^2 \chi}. \quad (42)$$

On the one side, this is the precise expression prescribed by Gauss’s theorem [18], and on the other, one recognizes in it the functional form of the Scarf well. As an important reminder, $V_{CD}(\chi)$ is conformal because the Green functions have the symmetry of the Laplacian, that on its side has the symmetry of the space-time on which it defines the kinetic energy operator.

One of the advantages of defining non-relativistic potentials in terms of Green functions is that elements of causality can be brought to the interactions through considering the retarded functions, a point that so far will not be attended here.

As a result, the hypothesis on the validity of dS_4 special relativity within the interaction domain [6] amounted to the prediction of the new phenomenon of conformally invariant charge neutral systems confined to closed hyper spherical spaces.

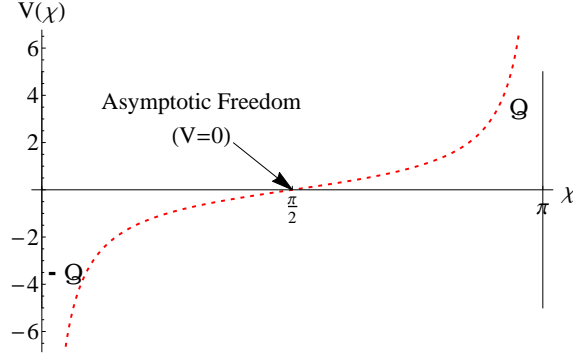


Figure 4: The conformal color dipole confining potential in the $\chi \in [0, \pi]$ parametrization.

The particular tangent form of the dipole potential is not universal but rather due to the choice of the parametrization for the second polar angle on S^3 , namely, $\chi \in [-\frac{\pi}{2}, +\frac{\pi}{2}]$. This choice is arbitrary and could be changed to $\chi \in [0, \pi]$ in which case the tangent goes into a cotangent and the \sec^2 into \csc^2 , as originally considered by [20]. From now onward we shall switch to this very parametrization which turns out to be more suited for physical interpretations, to be presented in the subsequent section.

Notice that \mathcal{Q} stands for dimension-less charges. In terms of dimensional charges, q , related to \mathcal{Q} via,

$$\mathcal{Q} = \frac{q}{\sqrt{\hbar c}}, \quad (43)$$

the potential perceived by another charge, $q/\sqrt{\hbar c}$, is

$$V(\chi) = \frac{q^2}{4\pi\hbar c\epsilon_0} \cot \chi, \quad \chi \in [0, \pi]. \quad (44)$$

For example, in the case of electrostatic, q is taken as the electron charge, e , in which case the special notation of,

$$\alpha = \frac{e^2}{4\pi\hbar c\epsilon_0} \quad (45)$$

known as the fundamental coupling constant of Electrodynamics, is introduced. In case the dipole is acting on a Ze charge, one finds the standard Coulomb interaction,

$$V_C^{(\alpha Z)}(\chi) = \alpha Z \cot \chi, \quad \chi \in [0, \pi]. \quad (46)$$

In Fig. 5 we display a dipole interaction, now in the $\chi \in [0, \pi]$ parametrization.

The potential in (44) can be applied as a perturbation of the free quantum motion on S^3 in (31), in which case the following wave equation emerges,

$$\mathcal{H}_{\text{Pert}}(\chi, \theta, \varphi) U_{\ell n}^{(\alpha Z)}(\chi) Y_{\ell m}(\theta, \varphi) = \frac{\hbar^2 c^2}{R^2} \left(\epsilon_{\ell n}^{(\alpha Z)} \right)^2 U_{\ell n}^{(\alpha Z)}(\chi) Y_{\ell m}(\theta, \varphi), \quad (47)$$

$$\mathcal{H}_{\text{Pert}}(\chi, \theta, \varphi) = \left(-\frac{\hbar^2 c^2}{R^2} \frac{d^2}{d\chi^2} + V_C^{(\alpha Z)}(\chi) \right) \mathbf{I}(\theta, \varphi), \quad (48)$$

$$V_C^{(\alpha Z)}(\chi) = V_{\text{Sc}}(\chi) + V(\chi) = \frac{\hbar^2 c^2}{R^2} \frac{\ell(\ell+1)}{\sin^2 \chi} - \alpha Z \frac{\hbar^2 c^2}{R^2} \cot \chi, \quad (49)$$

where $\mathbf{I}(\theta, \varphi)$ is the identity operator in the (θ, φ) variables. Because the perturbation of the free quantum motion on S^3 takes place only in the χ variable, while leaving intact the motion in the θ and φ variables, the $\mathcal{H}_{\text{Pert}}$ operator depends

non-trivially only on the χ variable and is in reality one-dimensional. The energies, $\frac{\hbar^2 c^2}{R^2} \left(\epsilon_{\ell n}^{(\alpha Z)} \right)^2$, of the states bound within this potential are known [13] and given in as,

$$\frac{\hbar^2 c^2}{R^2} \left(\epsilon_{\ell n}^{(\alpha Z)} \right)^2 = \frac{\hbar^2 c^2}{R^2} \left[-\frac{\alpha^2 Z^2}{4(K+1)^2} - (K+1)^2 \right],$$

$$K = \ell + n, \quad K = 0, 1, 2, \dots \quad (50)$$

The “spectral” mass formula resulting then from this potential reads,

$$M^2 = \frac{\hbar^2 c^2}{R^2} \left(\epsilon_{\ell n}^{(\alpha Z)} \right)^2 = \frac{\hbar^2 c^2}{R^2} (K+1)^2 - \frac{\hbar^2 c^2 \alpha^2 Z^2}{4R^2 (K+1)^2} + c_0. \quad (51)$$

In eqs. (47)-(49) one recognizes the one-dimensional wave equation with a version of the trigonometric Rosen-Morse potential, known from the super-symmetric quantum mechanics to be exactly solvable [13].

Identifying now the “charge” with the color charge, α is replaced by the QCD strong coupling, α_s , while Z is replaced by the number of colors, N_c [5],[8]. In this way, the following potential has been found,

$$V^{(\alpha_s N_c)}(\chi) = \frac{\hbar^2 c^2}{R^2} \frac{\ell(\ell+1)}{\sin^2 \chi} - \alpha_s N_c \frac{\hbar^2 c^2}{R^2} \cot \chi, \quad (52)$$

to be relevant in quark models. Correspondingly, the mass formula emerges as,

$$M^2 = \frac{\hbar^2 c^2}{R^2} \left(\epsilon_{\ell n}^{(\alpha_s N_c)} \right)^2 = \frac{\hbar^2 c^2}{R^2} (K+1)^2 - \frac{\hbar^2 c^2 \alpha_s^2 N_c^2}{4R^2 (K+1)^2} + c_0. \quad (53)$$

To recapitulate, the result is that in hypothesizing validity of dS_4 special relativity [6], it became possible to predict the form of a potential generated by equal numbers of charges and anti-charges locked (confined) on a closed hyper-spherical space, much alike the phenomenon of color confinement in QCD.

6 The experimental verification

The phenomenon of charge confinement predicted by the dS_4 special relativity in the previous section is well known from the theory of strong interactions, the Quantum Chromodynamics (QCD) [21], in which the fundamental matter degrees of freedom, the quarks, are endowed with so called “color” charges. There are three color charges, and three color anti-charges, although the strongly interacting particles, the hadrons, are by themselves all color charge neutral. For example, the hadrons of integer spin, the mesons, are constituted by effective degrees of freedom, termed to as “constituent” quarks, and “anti-quarks”, which are equipped by opposite color charges. Within this context it is legitimate to ask the question as to what extent the scenario developed in the preceding sections and especially of the previous section 5 could apply to the description of the experimentally reported meson masses. The question we are posing is as to what extent the dual “trajectory”- and “spectral” mass formulas in the respective eqs. (26), and (33) are suited for the description of the meson mass dependencies on their angular momenta. Such an analysis has been performed in [5] and we here limit ourselves to only briefly highlight the results.

In [5] we analyzed 71 reported unflavored mesons belonging to the four families of the f_0 , a_0 , π , and η mesons. Data convincingly confirmed the conformal hydrogen-like $(K+1)^2$ -fold degeneracy of the levels in accord with (53). In addition, their splittings followed pretty much those of the states bound within the trigonometric Scarf potential in (33). Also the dual mass formula in (26) turned out well applicable. The only splittings which could not come out well from the formulas under discussions were the splittings between the ground states and the first excited states. They could be accounted for by the help of the extension in (52).

Usage of (44) as a perturbation was justified by the suggestion to consider mesons as made of two types of color-dipoles, one constituted by a quark and an anti-quark, and the other by a gluon and an anti-gluon. The meson Hamiltonian, $\mathcal{H}_{\text{pert}}$, of such a system, given in (48), can then be approximately separated into a dominant free 4D rotational motion of say, the supposedly light quark-anti-quark pair, described by the Hamiltonian \mathcal{H}_{Sc} in (29), perturbed by the “residual” color-dipole interaction, $V_{CD}(\chi)$ in (44), generated by a background gluon-antigluon dipole. Such a picture is consistent with

the idea of the constituent quarks as effective degrees of freedom, i.e. as fundamental quarks “dressed” by gluons. In adopting $\mathcal{H}_{\text{Pert}}$ as a working hypothesis, one is of course neglecting the perturbation of the glueball by the color-dipole potential generated by the quark-anti-quark pair, and the tensor interaction between the two dipoles [22].

Notice that the interpretation of hadrons as states bound within a well potential is adequate near the rest frame, while their interpretation as resonances transmitted through a barrier is suited for high to ultra-relativistic energies. The rest frame is acceptable as an approximation at low transferred momenta in the so called infrared (IR) regime of QCD, while the adequate tool for hadron description at high-and ultra-high transferred momenta, i.e. close to the ultraviolet (UV) regime of QCD, is provided by the scattering matrix. Stated differently, within the QCD context, the quantum motions on the open time-like geodesics can be associated with processes approaching the ultraviolet regime, while those on the closed space-like geodesics can be associated with near rest frame processes, i.e. with the infrared regime of QCD. In this sense, the achievement of the model advocated in [5] is to have

- associated (to a good approximation) each one of the infrared and the ultraviolet regimes of QCD with free motions along the respective closed hyper-spherical space-like –, and the open hyperbolic time-like geodesics on a conformally symmetric dS_4 space-time,
- established with respect to meson description a duality between states bound within a well-(IR), and resonances transmitted through a barrier (UV) potentials,
- gained the new understanding about the inevitable color-neutrality of hadrons in the infrared as a consequence of the innate charge-neutrality of the closed hyper-spherical space-like dS_4 geodesics and predicted a confinement phenomenon known in QCD,
- revealed relevance of conformal symmetry in both regimes of QCD.

Notice that color-neutrality in the ultraviolet occurs by virtue of the dual meson description and is not inevitable there because on open space-times free charges and therefore a deconfined phase, are allowed to exist.

Finally, it needs to be emphasized that the infrared $(-\mathcal{Q}) \mathcal{G}_{\frac{\pi}{2}}(\chi)$ single-color potential in (40) relates by an argument shift toward, $\chi = \chi' + \pi/2$, followed by the complexification, $\chi' \rightarrow i\chi' \rightarrow \rho$, to the expression $(-\mathcal{Q}) (-i\chi') \cot i\chi' \rightarrow -(-\mathcal{Q}) \rho \coth \rho$, giving a single-color potential generated in the ultraviolet by a soft-gluon emission of a fast quark, stopped at a cusp [23], and in support of the IR-UV duality advocated here and in [5]. The Wilson loop calculation of such a potential, in making use of radial quantization, is practically equivalent to our calculation in section 5.

6.1 The spectra of the a_1 and f_1 mesons

As already mentioned above, the fundamental matter degrees of freedom in the theory of strong interaction, the Quantum Chromodynamics, the quarks, can carry three different color charges. The color charge, denoted by $g(Q^2)$, depends on the square, q^2 , of the transferred space-like four-momentum, via $Q^2 = -q^2$, and the related fundamental coupling in QCD, $\alpha_s(Q^2)$, defined in analogy to (45) as,

$$\alpha_s(Q^2) = \frac{g^2(Q^2)}{4\pi\hbar c}, \quad Q^2 = -q^2 \geq 0, \quad (54)$$

changes with Q^2 , a reason for which it is termed to as “running”.

In the following we complement the analyzes of the mass distributions of the four meson families previously studied in [5] (71 masses) by two more meson families, those of the f_1 , and a_1 mesons, which contribute 18 more masses. Afterwards we extract the corresponding α_s values. Compared to the f_0 , η , π , a_0 mesons, analyzed in [5], less is known about the f_1 and a_1 mesons. The compiled data on the last two families are presented in Fig. 5. It needs to be said that only the $a_1(1260)$, $a_1(1640)$, and $f_1(1285)$ mesons are contained in the Summary Table of the Meson Particle Listings in [1] meaning that their existence is considered as fully reliable. All the other particles in Fig. 5 are either included in the Meson Particle Listings, or into the list of the less reliably established particles referred to as “Further States”. We here favored the $f_1(1510)$ meson as the first excited state of $f_1(1285)$ over the $f_1(1420)$ state from the Summary Table. In this way we are suggesting that the internal $f_1(1510)$ structure may be closer to a quark–anti-quark color dipole, perturbed by the dipole potential due to gluon–anti-gluon dipole, than the $f_1(1420)$ internal structure, which may contain strange-anti-strange quarks. Our point is that our conformal symmetry classification scheme, in needing states omitted from the Summary Table, provides an additional legitimization to their observation and consolidates their status. Same as in [5], we here employ the mass formula in (53) to perform a least square fit to the meson mass distributions in Fig. 5. The results on the three parameters, the hyper-sphere radius, R , and the two dimensionless parameters b , and

trajectory	R	b	c_0	σ^2 [GeV] ⁴	$\frac{\alpha_s}{\pi}$
f_1 for $K \geq 0$	0.58 fm	3.788	5.125	0.1652839 GeV ⁴	0.80
a_1 for $K \geq 0$	0.58 fm	3.726	5.071	0.09191531 GeV ⁴	0.79

Table 1: Parameters of the least square fit to the 18 masses of the a_1 and f_1 mesons, distributed over the two trajectories indicated in the first column, and calculated employing the mass formula in (53). The last column contains the value of the extracted strong coupling constant, α_s/π , identified by the equation (53), with $2b = \alpha_s N_c$. The explicit expression of σ^2 reads $\sigma^2 = \frac{(\sum \Delta M^2)^2}{N-1}$, where ΔM^2 stands for the deviation of the squared experimental from the squared theoretical masses, and N is the number of states in a family.

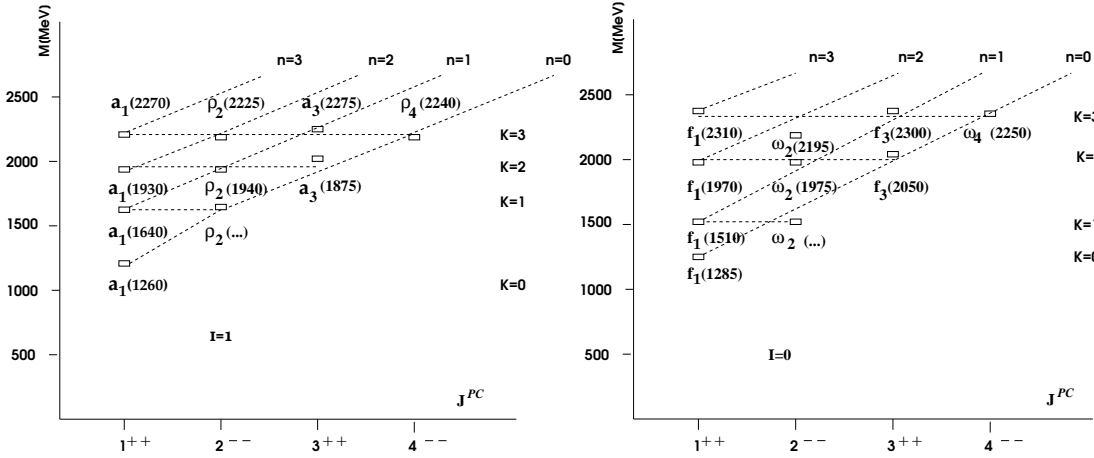


Figure 5: The excitations of the isovector $a_1(1260)$ meson (left) and the isoscalar $f_1(1285)$ meson (right). “Missing” states are denoted by (...). Here, J is the total angular momentum value of the quark-diquark system obtained from coupling the total spin $S = 1$, to the relative angular momentum, $\ell = 0, 1, 2, 3$, and CP give in their turn the C and P quantum numbers. Recall the definition of $K = n + \ell$ in (26).

c_0 in (53), are listed in the columns second to fourth of Table 1. The fifth column contains the average deviation values of the corresponding fits, while in the last column we present the values of the strong coupling constant, α_s of QCD (normalized to π) which we extracted by virtue of the formula (53). The Table shows that the two α_s/π values, in being of the order of $\alpha_s/\pi \sim 0.80$, remain significantly less than 1, and in complete agreement with data reported in [24], whose principle result is that the strong coupling constant tends to approach a fixed value in the infrared, thus opening up a so called “conformal window” and thereby hints on relevance of conformal symmetry in the infrared.

6.2 The electric form factor of the pion

In our previous work [10] we formulated on S^3 the Dirac equation with the color-confining dipole potential in (44), found the spinor solutions in closed forms, and used them in the calculations of the proton’s and neutron’s electric-charge, $G_{p/n}^E(Q^2)$, and magnetic dipole, $G_{p/n}^M(Q^2)$ form factors, together with the respective Dirac- and Pauli form factors, $F_1^{p/n}(Q^2)$, and $F_2^{p/n}(Q^2)$.

The electric charge form factor of the proton is determined by the Fourier transform of the electric-charge density, $\rho^p(\vec{r})$, as

$$G_p^E(Q^2) = \int_{V(\vec{r}) \rightarrow \infty} \rho^p(r) e^{i\vec{q} \cdot \vec{r}} d^3\vec{r}, \quad \rho^p(\vec{r}) = |\Psi_{gst}(\vec{r})|^2, \quad (55)$$

$$Q^2 = -q^2, \quad (56)$$

where Q^2 equals the negative squared of the transferred space-like momentum, $q^2 < 0$, $V(\vec{r})$ is the space integration

volume, and $\Psi_{gst}(\vec{r})$ is the Dirac spinor of ground state. The proton's magnetic dipole form-factor is given by the Fourier transform of the magnetic dipole density, $\rho_{mag}^p(\vec{r})$ as,

$$G_p^M(Q^2) = \int_{V(\vec{r}) \rightarrow \infty} \rho_{mag}^p(r) e^{i\vec{q} \cdot \vec{r}} d^3\vec{r}, \quad \rho_{mag}^p(\vec{r}) = \bar{\Psi}_{gst}(\vec{r}) \gamma_5 \Psi_{gst}(\vec{r}). \quad (57)$$

The relation between $G_p^E(Q^2)$, and $G_p^M(Q^2)$ to the Dirac and Pauli form factors, $F_1^p(Q^2)$, and $F_2^p(Q^2)$, is given by,

$$\begin{aligned} F_1^p(Q^2) &= \frac{G_p^E(Q^2) + \tau_p G_p^M(Q^2)}{1 + \tau_p}, \quad \tau_p = \frac{Q^2}{2M_p^2}, \\ \kappa_p F_2^p(Q^2) &= \frac{G_p^M(Q^2) - G_p^E(Q^2)}{1 + \tau_p}, \quad \kappa_p = \mu_p - 1, \end{aligned} \quad (58)$$

where μ_p is the proton's magnetic dipole moment. The neutron form factors are expressed by means of the proton's form factors as,

$$\begin{aligned} G_n^E(Q^2) &= -\frac{\mu_n \tau_n}{1 + B\tau_n} G_p^E(Q^2), \quad \tau_n = \frac{Q^2}{2M_n^2} \\ \frac{G_n^M(Q^2)}{\mu_n} &= \frac{G_p^M(Q^2)}{\mu_p}, \end{aligned} \quad (59)$$

where B is a parameter, while μ_n is the magnetic dipole moment of the neutron. In [10] expressions in closed form for all the above form-factors have been reported, which we opted not to repeat here for the sake of not overloading the presentation. On the other side, all the form factors can also be alternatively expressed in terms of the respective form factors of the constituent u and d quarks. Specifically for the Dirac and Pauli form factors the following expressions hold valid,

$$F_i^u(Q^2) = 2F_i^p(Q^2) + F_i^n(Q^2), \quad i = 1, 2, \quad (60)$$

$$F_i^d(Q^2) = F_i^p(Q^2) + 2F_i^n(Q^2). \quad (61)$$

These form factors, extracted from the $F_p^1(Q^2)$ and $F_n^2(Q^2)$ expressions reported in [10] are plotted in Fig. 6.

We observe that our predictions on the light quark form factors are of same quality as those reported in [25] and worked out within the framework of the related ADS_5/CFT_4 formalism. Knowing the quark form factors allows one to obtain the form factor $F_\pi(Q^2)$ of the positively charge pion, π^+ , as

$$F_\pi(Q^2) = \frac{1}{2} \left[\frac{2}{3} F_1^u(Q^2) \right] - \left[-\frac{1}{3} F_1^d(Q^2) \right], \quad (62)$$

where we maintained same potential parameters as those fitted to the proton's and neutron's form factors.

Here, the last term on the r.h.s. in the latter equation stands for the \bar{d} form factor. The satisfactory result, displayed in Fig. 7 together with its comparison with data taken from [26], provides a further support for the convenience of our suggested approach to hadron spectroscopy.

7 Conclusions

Our analyzes show that the experimentally reported conformal symmetry patterns of the light flavored meson mass distributions are well modelled by a conformal dS_4 internal space-time, considered as located outside of the Minkowskian light cones attached to local observers on this space, and hypothesized as the geometry relevant for the description of the virtual degrees of freedom inside hadrons. Along this line, the interaction in the infrared regime of QCD among the virtual hadron constituents has been defined by the Laplacian of the closed space-like hyper-spherical geodesics S^3 on dS_4 , where quark and gluon systems are inevitably and necessarily colorless. In effect, hadrons in the infrared have been viewed as color-anti-color dipoles in free conformal four-dimensional quantum rotation, described by the $\ell(\ell+1)\csc^2\chi$ potential, or, rotation slightly perturbed by the also conformal color-dipole potential, $(-\alpha_s N_c \cot \chi)$, attributed to a gluon-anti-gluon color dipole. The magnitude of the perturbation is proportional to the product of the number of colors,

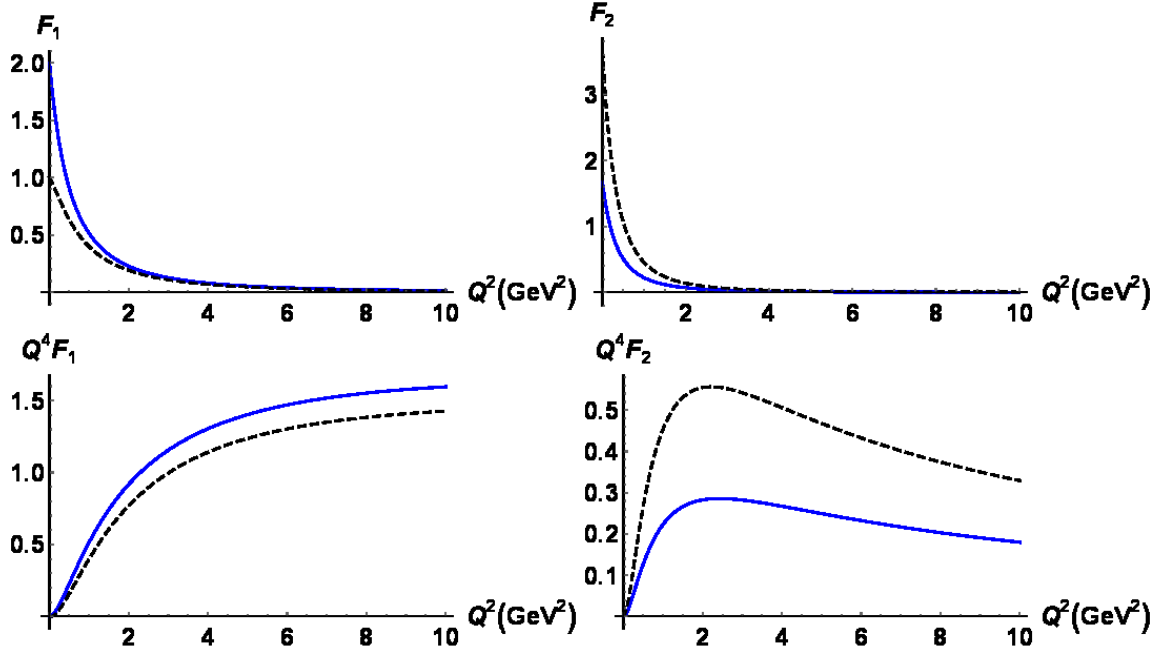


Figure 6: The Dirac and Pauli form factors of the u (solid lines) and d (dashed lines) quarks (left and right top figures), and their respective scalings (left and right bottom figures).

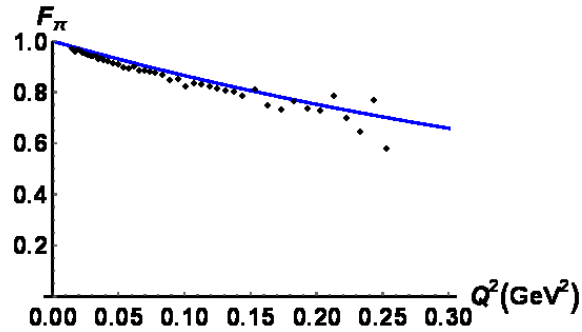


Figure 7: The pion electric form factor, $F_\pi(Q^2)$, calculated with the aid in (62) (solid line) in comparison to data taken from [26] (dots).

N_c by the strong coupling constant, α_s , by virtue of (52), a circumstance that allowed us to extract from data on meson masses reasonable α_s -values, and to conclude on the relevance of a dynamical conformal symmetry in both the extreme regimes of QCD.

Thus, the dynamical conformal symmetry, via dS_4 special relativity, backs up the internal color gauge group, $SU(3)_C/Z_3$, in QCD. However, on open spaces, be them the open time-like geodesics on dS_4 , or its casual patches, on which no charge-neutrality is required, color excess could exist within this scenario and become detectable. Our findings favor a space-time, with one extra (infinite) dimension in the internal coordinate space. The scheme is Fourier transformable and can be re-formulated in momentum space. Models of this type are free from infrared divergences [23], a reason for which considering QCD on closed spaces is appealing (also see [4] for further reading). To the best of our knowledge, the model under discussion is so far the only one which allows to estimate the fundamental coupling constant of QCD from analyzes of global (integral) properties of hadron systems such as spectra. Usually, these values are extracted from data on the spin structure function [24]. Our major conclusion is that behind the curtains of conformal symmetry and color-confinement in QCD one may encounter the deSitter dS_4 special relativity as a string-puller. Finally, the quality reached in the description of the electromagnetic form factor of the pion indicates that the u quark in the pion is same as in the proton, while the \bar{d} quark in the pion is related to the d quark in the proton by charge conjugation.

References

- [1] K. A. Olive *et al.* (Particle Data Group), Review of Particle Physics, Chinese Physics C **38** 090001 (2014) and 2015 update.
- [2] Fayyazuddin and Riazuddin, *A Modern Introduction to Particle Physics*, 2nd edition (World Scientific, Singapore, 2000)
- [3] A. Chodos, R. L. Jaffe, K. Johnson, and C. B. Thron, Phys. Rev. D **10** (1974) 2599.
- [4] D. Kharzeev, E. Levin, and K. Tuchin, Phys. Rev. D **70** (2004) 054005 .
- [5] M. Kirchbach and C. B. Compean, Eur.Phys.J. A **52** (2016) 210.
- [6] R. Aldrovandi, J. P. Beltrán Almeida, and J. G. Pereira, Class. Quant. Grav. **24** (2007) 1385.
- [7] O. D. Kellogg, *Foundations of Potential Theory* (Dover, New York, 1953).
- [8] M. Kirchbach and C. B. Compean, Eur.Phys.J. A **53** (2017) 65.
- [9] A. O. Barut and R. Wilson, Phys. Lett. A **110** (1983) 351.
- [10] M. Kirchbach and C. B. Compean, Nucl. Phys. A **980** (2018) 32.
- [11] Slava Rychkov, *EPFL Lectures on Conformal Field Theory in $D \geq 3$ dimensions*, E-print arXiv:1601.05000[hep-th].
- [12] Yoonbai Kim, Chae Young Oh, and Namil Park, J. Korean Phys. Soc. **42** (2003) 573 .
- [13] F. Cooper, A. Khare, and U. P. Sukhatme, *Supersymmetry in Quantum Mechanics* (World Scientific, Singapore, 2001).
- [14] Andrew Pressley, *Elementary Differential Geometry* (Springer, London Dordrecht Heidelberg New York, 2012).
- [15] D. Cevik, M. Gadella, S. Kuru, and J. Negro, Phys. Lett. A **380** (2016) 1600.
- [16] H. Bateman, Proc. London Math. Soc. (ser. 2) **7** (1909) 70.
- [17] L. D. Landau and E. M. Lifschitz, *The Classical Theory of Fields*, Vol. 2 of A Course of Theoretical Physics, 3d edition (Pergamon Press 1971) p.335.
- [18] Pouria Pedram, Am. J. Phys. **78** (2010) 403.
- [19] S. Fubini, A. J. Hanson, and R. Jackiw, Phys. Rev. D **7** (1972) 1732.
- [20] B. Alert, Ann.Inst.Henri Poincaré, **53** (1990) 319.
- [21] Kerson Huang, *Quarks, Leptons and Gauge Fields* (World Scientific, Singapore, 1982).
- [22] J.-M. Gaillol and M. Trulsson, J. Chem. Phys. **141** (2014) 124111.
- [23] A. V. Belitsky, A. S. Gorsky, and G. P. Korchemsky, Nucl. Phys. B **67** (2003) 3.

- [24] A. Deur, V. Burkert, J. P. Chen, and W. Korsch, Phys. Lett. **665** (2008) 349.
- [25] Dipankar Chakrabart, Chandan Mondal, Eur. Phys. J. C **73** (2013) 2671.
- [26] S. R. Amendolia et al., Nucl. Phys. B 277 (1986) 168.